

# Growth of InP on GaAs (001) by hydrogen-assisted low-temperature solid-source molecular beam epitaxy

P. A. Postigo<sup>a)</sup> and F. Suárez

*Instituto de Microelectrónica de Madrid, Centro Nacional de Microelectrónica, Consejo Superior de Investigaciones Científicas, Isaac Newton 8, PTM Tres Cantos, 28760, Madrid, Spain*

A. Sanz-Hervás and J. Sangrador

*Departamento de Tecnología Electrónica, E.T.S.I. Telecomunicación, Universidad Politécnica de Madrid, Ciudad Universitaria, 28040 Madrid, Spain*

C. G. Fonstad

*Department of Electrical Engineering and Computer Science, and Microsystems Technology Laboratory, Massachusetts Institute of Technology, Cambridge, Massachusetts 02139, USA*

(Received 18 July 2007; accepted 7 November 2007; published online 9 January 2008)

Direct heteroepitaxial growth of InP layers on GaAs (001) wafers has been performed by solid-source molecular beam epitaxy assisted by monoatomic hydrogen ( $H^*$ ). The epitaxial growth has been carried out using a two-step method: for the initial stage of growth the temperature was as low as 200 °C and different doses of  $H^*$  were used; after this, the growth proceeded without  $H^*$  while the temperature was increased slowly with time. The incorporation of  $H^*$  drastically increased the critical layer thickness observed by reflection high-energy electron diffraction; it also caused a slight increase in the luminescence at room temperature, while it also drastically changed the low-temperature luminescence related to the presence of stoichiometric defects. The samples were processed by rapid thermal annealing. The annealing improved the crystalline quality of the InP layers measured by high-resolution x-ray diffraction, but did not affect their luminescent behavior significantly. © 2008 American Institute of Physics. [DOI: 10.1063/1.2824967]

## I. INTRODUCTION

The integration of microelectronics and optoelectronic devices has been and still is an important goal in semiconductor technology. Wafer bonding techniques have been used to produce Si and GaAs substrates compatible with the monolithic integration of III–V heterostructures.<sup>1</sup> GaAs wafers have been used to integrate electronic and optoelectronic devices monolithically on the same substrate.<sup>2</sup> InP-based devices have already shown compelling performance advantages over GaAs for laser, light-emitting devices (LED), and wireless applications. InP-related devices are even now entering the mainstream of commercial integrated circuit production. However, a drawback of InP-based technology is the substrate itself. InP is a brittle material and its production is not as mature as that of GaAs. This limits the InP wafer size and its crystalline quality. Therefore, the cost per square inch of InP wafers is relatively high. In order to combine the advantages of GaAs substrates with the benefits of InP-based devices, metamorphic technology is one of the appropriate ways to extend the range of GaAs into InP territory, especially for large-scale and low-cost device fabrication.<sup>3–6</sup> However, there is a large lattice mismatch (3.8%) between InP and GaAs, which makes the heteroepitaxy very difficult.<sup>7,8</sup> Matthews and Blakeslee's theoretical expression<sup>9</sup> predicts that the critical thickness for a 3.8% lattice mismatch is lower than 5 nm. Numerous threading and misfit dislocations will come about once the critical film thickness

is reached, thus hindering the realization of well-performing devices. Efforts have been made in the pursuit of growing high-quality buffer layers to suppress dislocations, such as strained-layer superlattice (SLS),<sup>10,11</sup> two-step,<sup>12,13</sup> graded,<sup>14</sup> or compliant substrate (CS)<sup>15,16</sup> methods. Metamorphic devices have been achieved by molecular beam epitaxy (MBE)<sup>17,18</sup> or by metalorganic vapor phase epitaxy (MOVPE).<sup>19–23</sup> On the other hand, the introduction of hydrogen by plasma treatment after growth has been shown to passivate dislocations on MOVPE-grown InP layers on GaAs (001) wafers<sup>24</sup> and to enhance the luminescent properties of CS InP layers on GaAs.<sup>25</sup> Moreover, hydrogen introduced during MOVPE growth produces a substantial decrease of deep-level traps.<sup>26</sup> It is known that monoatomic hydrogen ( $H^*$ ) affects the optical properties of semiconductors by strong carrier passivation;<sup>26</sup> a postgrowth annealing at temperatures above 400 °C produces an immediate recovery. It is also known that rapid thermal annealing (RTA) of heteroepitaxial InP layers at 780 °C enhances their optical properties.<sup>27</sup>

In this work, we use low-temperature (200–480 °C) solid-source molecular beam epitaxy and a two-step method to grow 2  $\mu\text{m}$  thick InP layers directly on GaAs (001) substrates. Monoatomic hydrogen has been introduced during the initial stages of growth. After growth, the samples have been processed by RTA. We will show that the crystalline and luminescent properties of the InP layers are good. The incorporation of  $H^*$  affects their luminescent properties, and the crystalline quality is improved by RTA, although RTA does not modify substantially their luminescent behavior.

<sup>a)</sup>Electronic mail: aitor@imm.cnm.csic.es.

TABLE I. Results from the HRXRD study:  $a_{\perp}$  (InP) is the perpendicular lattice parameter for the InP layers;  $R$  is the relaxation coefficient of the InP layers; rc FWHM is the average rocking-curve FWHM around the 002 and 004 reflections of InP;  $\Delta$ FWHM is the relative change of the InP rc FWHM after RTA; and  $a_{\perp}$  (GaAs) is the perpendicular lattice parameter of the GaAs substrate. Numbers in parentheses indicate the uncertainty ( $\sigma$ ) of the measurements.

Sample	$a_{\perp}$ (InP) (Å)	$R$ (%)	rc FWHM ( $^{\circ}$ )	$\Delta$ FWHM (%)	$a_{\perp}$ (GaAs) (Å)
No H*	5.8739(5)	99.8(1)	607(5)	-	5.6529(4)
No H* after RTA	5.8777(5)	99.6(1)	431(4)	-29	5.6537(4)
BEP(H*) = $1 \times 10^{-5}$ mbar	5.8744(5)	99.1(1)	704(5)	-	5.6536(4)
BEP(H*) = $1 \times 10^{-5}$ mbar after RTA	5.8772(5)	99.7(1)	517(4)	-26	5.6530(4)
BEP(H*) = $5 \times 10^{-5}$ mbar	5.8741(5)	99.1(1)	689(5)	-	5.6540(4)
BEP(H*) = $5 \times 10^{-5}$ mbar after RTA	5.8773(5)	99.6(1)	496(4)	-28	5.6534(4)

## II. SAMPLE GROWTH AND RAPID THERMAL ANNEALING

Growth was carried out in a MBE system equipped with a filament hydrogen cracker kept at  $T_H \sim 2000$  °C and a GaP-decomposition source for the production of a molecular beam of  $P_2$ .<sup>28</sup> GaAs (001) semi-insulating substrates were used for the growth of the InP layers. Oxide desorption of GaAs was made without As under a H\* flux with a beam equivalent pressure (BEP) of H\* of  $1 \times 10^{-5}$  mbar. The sample was kept at a maximum temperature of 475 °C for 50 min, showing a bright ( $2 \times 4$ ) reflection high-energy electron diffraction (RHEED) pattern with long diffraction lines, typical of a flat surface. This favorable behavior allowed us to avoid the growth of a conventional GaAs buffer layer. The sample was then cooled down to 200 °C under the same flux of H\*. A clear ( $2 \times 2$ ) reconstruction pattern was observed. The growth of InP was started under these conditions with a growth rate of 0.5 ML/s and a  $P_2$  flux of  $1 \times 10^{-6}$  mbar. After 3.5 min (corresponding to a nominal thickness of 30 nm) the RHEED pattern changed to a bright ( $2 \times 1$ ) pattern with long lines. After 8 min from the beginning of the growth of the InP layer (thickness of 70 nm), the reconstruction along the  $[1-10]$  direction turned a bit hazy. The lines became only slightly broken after 15 min of growth, but still resembled lines. Thirty minutes after growth was started (thickness of 264 nm) and still with a ( $2 \times 1$ ) pattern, the H\* flux was stopped and the substrate temperature was increased 1 °C/min until  $T_s = 480$  °C. The ( $2 \times 4$ ) reconstruction was visible from the moment  $T_s = 450$  °C was reached. InP was grown under these conditions to a total thickness of 2  $\mu$ m. For comparison, we have grown an InP layer on GaAs (001) under the same conditions but without H\*. In this case, the RHEED became spotty after only 50 s of InP growth, which corresponds to a thickness of 7.3 nm, close to the value predicted by the Matthews and Blakeslee's model.<sup>9</sup> The RHEED pattern after 20 min was fully spotty and very dark. The growth was completed under these conditions to a total thickness of 2  $\mu$ m. In all the cases the samples were slowly cooled down to room temperature at a rate of 2 °C/min under a  $P_2$  flux.

The heteroepitaxial samples were processed by RTA in a chamber purged with flowing nitrogen. The peak temperature was 780 °C and the ramp-up time was 10 s.<sup>27</sup> The cooling of the sample took about 15 s. To prevent phosphorous loss, a

200 nm thick  $SiO_x$  layer deposited by low-temperature plasma-enhanced chemical vapor deposition was added before the RTA processing. After RTA, the surface of the samples had not suffered any damage.

## III. EX SITU CHARACTERIZATION TECHNIQUES

All the samples were studied by high-resolution x-ray diffraction (HRXRD) after the epitaxial growth and after the RTA treatment to determine their crystalline quality and strain status. The HRXRD study was conducted with a Bede D<sup>3</sup> diffractometer using monochromatic Cu  $K\alpha_1$  radiation. We recorded  $\theta/2\theta$  scans and rocking curves (rc) around the symmetrical 002 and 004 and the asymmetrical 115 reflections of InP and GaAs. The 115 reflections were measured both in low-angle and high-angle incidence geometries. All this allowed us to measure the in-plane and perpendicular strains, from which we derived the lattice constants of GaAs and InP and the relaxation coefficient of the InP layers. The detector aperture was 0.2° for the  $\theta/2\theta$  scans and 1.5° for the rocking curves. A maximum angular step of 0.01° was used for the  $\theta/2\theta$  measurements. To obtain the full width at half-maximum of the rc (rc FWHM) and the peak maximum angle with good accuracy, each peak was fitted using a Gaussian function.

Room-temperature and low-temperature PL was measured on the same samples using a lock-in setup with a chopped Ar laser for excitation and a liquid nitrogen cooled Ge detector on a 0.22 m spectrometer with a resolution of  $\sim 0.4$  nm. An intermediate intensity of excitation (60 W/cm<sup>2</sup>) was used.

## IV. RESULTS AND DISCUSSION

Table I summarizes the main results from the HRXRD study. The perpendicular lattice parameters  $a_{\perp}$  for InP and GaAs were deduced from the Bragg angles of the 002 and 004 reflections of each material. As a check of the accuracy of the measurements, it can be seen that the values of  $a_{\perp}$  (GaAs) are very close to the accepted value<sup>29</sup> of 5.653 25(2) Å (the number in parentheses indicates the mean standard deviation  $\sigma$  of the measurements). The perpendicular lattice parameter of the InP layers before RTA is  $a_{\perp}$  (InP)  $\approx 5.8741(5)$  Å, a value slightly larger than other published values for InP [5.8687(10) Å in Ref. 29]. A sec-

ondary ion mass spectrometry analysis of our samples has revealed a content of As of 1.6%, typically associated with a residual background of As in the MBE chamber. This content of As is compatible with the measured values of  $a_{\perp}$ (InP). The HRXRD asymmetrical 115 reflections show that all the InP layers are almost fully relaxed. The hydrogenated layers still preserve some in-plane stress ( $R=99.1\%$ ), while the nonhydrogenated InP layer is fully relaxed ( $R=99.8\%$ ). The rc FWHM values for InP shown in the table were obtained as an average of the FWHM values of the rocking curves around the 002 and 004 reflections. The rc FWHM for the sample without  $H^*$  is clearly smaller than for the samples grown with  $BEP(H^*)$  of  $1 \times 10^{-5}$  and  $5 \times 10^{-5}$  mbar. It seems, therefore, that H incorporation partially inhibits stress relaxation. This might produce a less homogeneous strain distribution that would explain the wider rc of the hydrogenated InP layers. As far as we know, the rc FWHM of our heteroepitaxial InP layers is similar, but not better, than other published results for  $\sim 2 \mu\text{m}$  thick layers.<sup>23,27</sup>

The results in Table I show that the InP lattice parameter  $a_{\perp}$ (InP) increases slightly after RTA in the three heteroepitaxial samples, with a value of  $a_{\perp}$ (InP)  $\approx 5.8774(5)$  Å. This increase is compatible with the appearance of thermal stress due to the difference between the linear thermal expansion coefficients of GaAs and InP (larger for GaAs). However, the most noticeable effect is a decrease of the rc FWHM of more than 25% with respect to the samples that were not annealed. A similar effect was reported previously.<sup>27</sup> Rocking curves measure the angular dispersion of the crystallographic planes; thus, the observed decrease indicates that the material has undergone some rearranging, resulting in a better crystalline quality. RTA also seems to favor the relaxation of the hydrogenated InP layers, whose relaxation coefficient rises to 99.6% after RTA. Thus, RTA has the expected effect of increasing the mobility of dislocations located at the InP/GaAs interface and in the InP bulk through the supply of thermal energy; this favors stress relaxation (larger  $R$ ) and produces a more uniform strain distribution (narrower rocking curve).

Figure 1 shows the low-temperature PL (20 K) spectra of the nonhydrogenated and hydrogenated InP layers on (001) GaAs and an InP homoepitaxial layer grown under the same conditions but without  $H^*$ . All the PL spectra shown in this paper have the same scale for the PL intensity because they have been measured under the same experimental conditions; so, to compare the spectra between different figures, it is only necessary to take into account the scaling factor that appears in them. For the heteroepitaxial samples there are three well-defined transitions at  $\sim 1.34$ ,  $\sim 1.37$ , and  $\sim 1.41$  eV. All the transitions are slightly shifted toward lower energies with respect to pure InP due to a slight incorporation of As during growth. The first transition at  $\sim 1.34$  eV has been observed in undoped homoepitaxial InP grown by MBE and MOCVD under specific conditions of growth; it has been related to a complex defect incorporating a phosphorus vacancy in InP.<sup>30–32</sup> The second transition ( $\sim 1.37$  eV) is related to a donor-band (DB) transition associated with a stoichiometric defect produced by an excess of phosphorous in solid-source MBE-grown InP at low temperature.<sup>33</sup> Despite the low flux of  $P_2$  used in this work,

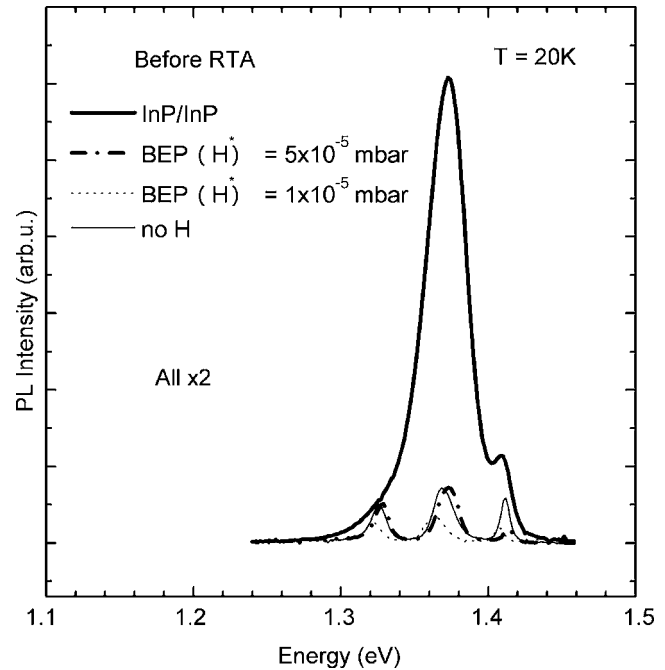


FIG. 1. Low-temperature PL (20 K) spectra of hydrogenated InP layers ( $H^*$  BEPs of  $1 \times 10^{-5}$  and  $5 \times 10^{-5}$ ), a nonhydrogenated heteroepitaxial layer, and an InP homoepitaxial layer grown without  $H^*$  under the same conditions as the other samples.

the low temperature used for most of the growth and the very high  $P_2/P_4$  ratio produced by the GaP decomposition cell<sup>28</sup> are sufficient to produce this P-related defect, which is very prominent in the case of the homoepitaxy.

The band-to-band (BB) transition at  $\sim 1.41$  eV is shifted by  $\sim 0.1$  meV toward lower energies due to the As incorporation. This transition has the highest intensity for the sample without  $H^*$ , for which it is almost half as intense as for the homoepitaxial InP grown under the same conditions. It is less intense for the hydrogenated samples.

The peaks at  $\sim 1.34$  and  $\sim 1.37$  eV do not follow a trend with  $H^*$  flux either. They have a similar intensity for  $BEP(H^*)=0$  or  $5 \times 10^{-5}$  mbar, whereas for  $BEP(H^*)=1 \times 10^{-5}$  mbar the intensity decreases, suggesting that there is an upper limit for the flux of  $H^*$  that helps to reduce the number of defects.

Figure 2 shows the PL spectra of the InP layers after RTA, measured under the same conditions as in Fig. 1. Now the hydrogenated sample with  $H^*$  [ $BEP(H^*)=1 \times 10^{-5}$  mbar] displays a clear BB peak whose intensity is about one third of the intensity of the InP homoepitaxy. The sample with  $BEP(H^*)=5 \times 10^{-5}$  mbar has a smaller intensity, whereas the heteroepitaxy without  $H^*$  almost does not emit photons at this energy. This indicates some beneficial effects of introducing  $H^*$  during the heteroepitaxial growth of InP on GaAs. Nevertheless, the defect-related peak at 1.37 eV increases drastically for the hydrogenated samples, with an intensity even higher than for the homoepitaxy for the sample with  $BEP(H^*)=1 \times 10^{-5}$  mbar, which suggests that a large concentration of radiative defects at this energy is created due to  $H^*$ .

Figure 3 shows the PL spectra at room temperature before RTA. The band gap transition of InP at 1.34 eV (again

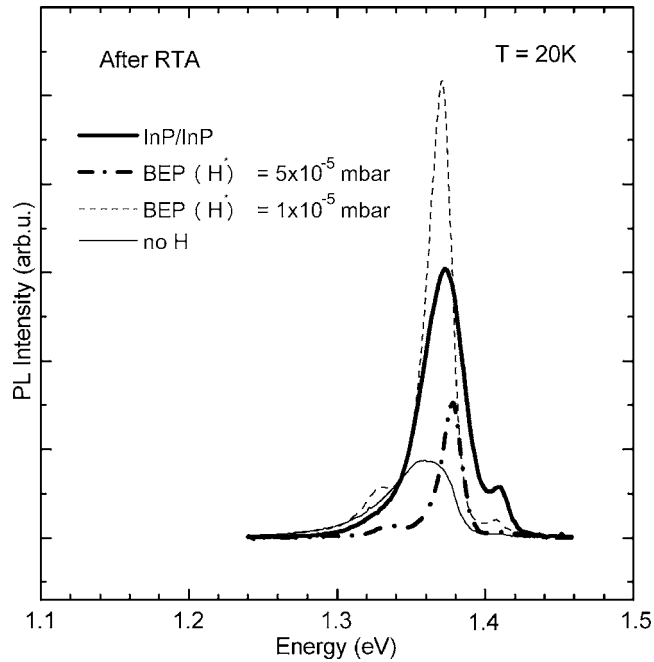


FIG. 2. PL spectra at low temperature (20 K) after RTA of the same samples of Fig. 1.

shifted by  $\sim 0.1$  eV to lower energy due to the residual presence of As) is clearly visible for all the samples. For the heteroepitaxies, the maximum intensity is for a  $H^*$  dose of  $BEP(H^*) = 1 \times 10^{-5}$  mbar, corresponding to almost one fourth of the intensity of homoepitaxial InP. A higher amount of  $H^*$  [ $BEP(H^*) = 5 \times 10^{-5}$  mbar] does not improve the quality, but rather produces a decrease of the PL intensity of about half of the value measured for the nonhydrogenated sample.

Figure 4 shows the PL measured under the same condi-

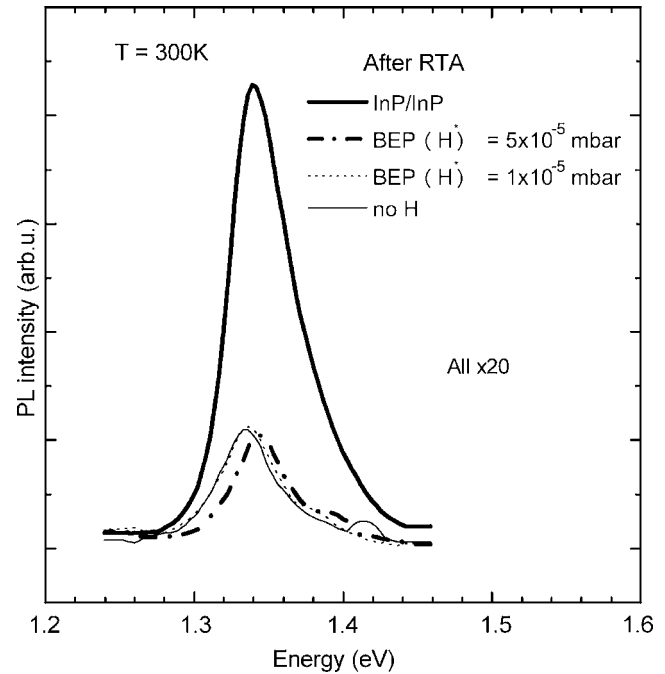


FIG. 4. PL spectra at room temperature after RTA.

tions but after RTA. In this case the intensity of the PL does not vary too much between hydrogenated samples and is around the same as for the hydrogenated sample with  $BEP(H^*) = 1 \times 10^{-5}$  mbar but before RTA. This means that the right dose of  $H^*$  introduced during MBE growth may produce a similar effect as RTA processing for this kind of heteroepitaxy.

## V. CONCLUSIONS

Heteroepitaxial layers of InP on (001) GaAs have been grown by solid-source molecular beam epitaxy assisted by monoatomic hydrogen in the first stages of the growth. The layers show good structural and optical properties, with a band-to-band PL intensity at room temperature of nearly one fourth of the intensity for the homoepitaxial InP grown under the same conditions. The effect of monoatomic hydrogen is twofold: on the one hand, it decreases band-to-band emission and increases radiative recombinations. On the other hand, it clearly enlarges the critical thickness of the InP layers as observed by RHEED, at least up to 200 nm, which is about 40 times the critical thickness predicted by Matthews and Blakeslee's model. The structural properties of the layers measured by HRXRD are enhanced by RTA, as expected, but for the right dose of hydrogen no RTA is needed in order to obtain the same PL at room temperature, which is remarkable. Further work is needed to test whether the use of monoatomic H during all the epitaxial growth may produce better heteroepitaxial layers.

## ACKNOWLEDGMENTS

The authors acknowledge support from the European Network of Excellence IST-2-511616-NOE (PHOREMOST) and NMP4-CT-2004-500101 (SANDIE), Spain-Italy Integrated Action HI2004-0367/IT2304, Projects NAN2004-

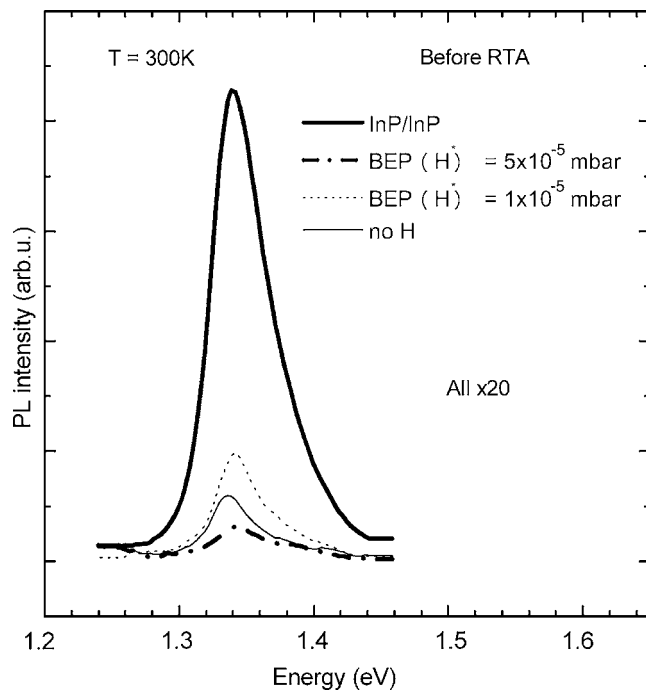


FIG. 3. PL spectra at room temperature before RTA.



08843-C05-04, TEC-2005-05781-C03-01, NAN2004-09109-C04-01, and CONSOLIDER-Ingenio 2010 (CSD2006-00019).

- <sup>1</sup>J. M. London, P. A. Postigo, and C. G. Fonstad, *Appl. Phys. Lett.* **75**, 3452 (1999).
- <sup>2</sup>P. A. Postigo, S. S. Choi, W. D. Goodhue, and C. G. Fonstad, *Appl. Phys. Lett.* **77**, 3842 (2000).
- <sup>3</sup>H. Wang, G. I. Ng, H. Zheng, H. Yang, Y. Xiong, S. Halder, K. Yuan, C. L. Tan, K. Radhakrishnan, and S. F. Yoon, *IEEE Trans. Electron Devices* **48**, 2671 (2001).
- <sup>4</sup>I. J. Fritz, B. E. Hammons, A. J. Howard, T. M. Brennan, and J. A. Olsen, *Appl. Phys. Lett.* **62**, 919 (1993).
- <sup>5</sup>Y. Mihasashi, K. Goto, E. Ishimura, M. Miyashita, T. Shimura, H. Nishiguchi, T. Kimura, T. Shiba, and E. Omura, *Jpn. J. Appl. Phys.* **33**, 2599 (1994).
- <sup>6</sup>J. C. P. Chang, J. Chen, J. M. Fernandez, H. H. Wieder, and K. L. Kavanagh, *Appl. Phys. Lett.* **60**, 1129 (1992).
- <sup>7</sup>F. Salomonsson, K. Streubel, J. Bentell, M. Hammar, D. Keiper, R. Westphalen, J. Piprek, L. Sagalowicz, A. Rudra, and J. Behrend, *J. Appl. Phys.* **83**, 768 (1998).
- <sup>8</sup>M. Chang, S. K. Mathis, G. E. Beltz, and C. M. Landis, *Mater. Res. Soc. Symp. Proc.* **535**, 9 (1999).
- <sup>9</sup>J. W. Matthews and A. E. Blakeslee, *J. Cryst. Growth* **27**, 118 (1974).
- <sup>10</sup>S. N. G. Chu, W. T. Tsang, T. H. Chiu, and A. T. Macrander, *J. Appl. Phys.* **66**, 520 (1989).
- <sup>11</sup>K. Hayashida, Y. Takagi, K. Samonji, H. Yonezu, M. Yokozeki, N. Ohshima, and K. Pak, *Jpn. J. Appl. Phys.* **34**, L1442 (1995).
- <sup>12</sup>Y. Takano, T. Sasaki, Y. Nagaki, K. Kuwahara, S. Fuke, and T. Imai, *J. Cryst. Growth* **169**, 621 (1996).
- <sup>13</sup>M. Akiyama, Y. Kawarada, and K. Kaminishi, *J. Cryst. Growth* **68**, 21 (1984).
- <sup>14</sup>H. Wang, G. I. Ng, H. Zheng, Y. Z. Xiong, L. H. Chua, K. Yuan, K. Radhakrishnan, and S. F. Yoon, *IEEE Electron Device Lett.* **21**, 427 (2000).
- <sup>15</sup>F. E. Ejeckam, M. L. Seaford, Y. H. Lo, H. Q. Hu, and B. E. Hammons, *Appl. Phys. Lett.* **71**, 776 (1997).
- <sup>16</sup>P. Chavarkar, L. Zhao, S. Keller, A. Fisber, C. Zheng, J. S. Speck, and U. K. Mishra, *Appl. Phys. Lett.* **75**, 2253 (1999).
- <sup>17</sup>K. C. Hwang, P. C. Chao, C. Creamer, K. B. Nichols, S. Wang, D. Tu, W. Kong, D. Dugas, and G. Patton, *IEEE Electron Device Lett.* **20**, 551 (1999).
- <sup>18</sup>W. E. Hoke, P. J. Lemonias, T. D. Kennedy, A. Torabi, E. K. Tong, R. J. Bourque, J. H. Jang, G. Cueva, D. C. Dumka, I. Adesida, K. L. Chang, and K. C. Hsieh, *J. Vac. Sci. Technol. B* **19**, 1505 (2001).
- <sup>19</sup>T. Kimura, T. Kimura, E. Ishimura, F. Uesugi, M. Tsugami, K. Mizuguchi, and T. Murotani, *J. Cryst. Growth* **107**, 827 (1991).
- <sup>20</sup>Y. Mihasashi, K. Goto, E. Ishimura, M. Miyashita, T. Shimura, H. Nishigushi, T. Kimura, T. Shiba, and E. Omura, *Jpn. J. Appl. Phys.* **33**, 2599 (1994).
- <sup>21</sup>A. Yoshikawa, T. Sugino, A. Nakamura, G. Kano, and I. Teramoto, *J. Cryst. Growth* **93**, 532 (1988).
- <sup>22</sup>C.-I. Liao, K.-F. Yarn, C.-L. Lin, Y.-L. Lin, and Y.-H. Wang, *Jpn. J. Appl. Phys.* **42**, 4913 (2003).
- <sup>23</sup>M. B. Derbali, J. Meddeb, H. Mâaref, D. Buttard, P. Abraham, and Y. Monteil, *J. Appl. Phys.* **84**, 503 (1998).
- <sup>24</sup>B. Chatterjee, S. A. Ringel, R. Sieg, R. Hoffman, and I. Weinberg, *Appl. Phys. Lett.* **65**, 58 (1994).
- <sup>25</sup>S. Balasubramanian, N. Balasubramanian, and V. Kumarg, *Semicond. Sci. Technol.* **10**, 310 (1995).
- <sup>26</sup>Y. F. Chen, K. C. Sung, W. K. Chen, and Y. S. Lue, *J. Appl. Phys.* **71**, (I), 509 (1992).
- <sup>27</sup>F. Riesz, K. Rakennus, T. Hakkarainen, and M. Pessa, *J. Vac. Sci. Technol. B* **9**, 176 (1991).
- <sup>28</sup>P. A. Postigo, G. Lullo, K. H. Choy, and C. G. Fonstad, *J. Vac. Sci. Technol. B* **17**, 1281 (1999).
- <sup>29</sup>*Semiconductors. Group IV Elements and III-V Compounds*, edited by O. Madelung (Springer-Verlag, Berlin, 1991).
- <sup>30</sup>A. A. Iliadis and S. Ovadia, *J. Appl. Phys.* **63**, 5460 (1988).
- <sup>31</sup>P. W. Yu, *J. Appl. Phys.* **48**, 5043 (1977).
- <sup>32</sup>B. Wakefield, L. Eaves, K. A. Prior, A. W. Nelson, and G. D. Davies, *J. Phys. D* **17**, L133 (1984).
- <sup>33</sup>P. A. Postigo, M. L. Dotor, P. Huertas, D. Golmayo, and F. Briones, *J. Appl. Phys.* **77**, 402 (1995).